Publications of the Korean Astronomical Society
32: 045 ∼ 047, 2017 March

pISSN 1225-1534
eISSN 2287-6936
https://doi.org/10.5303/PKAS.2017.32.1.045

AN EXTENSION OF A RELIABLE WAVELENGTH COVERAGE OF THE AKARI NG GRISM MODE

Shunsuke Baba[1,2], Takao Nakagawa[1], Naoki Isobe[1], Mai Shirahata[3], Youichi Ohyama[4], Kenichi Yano[1,2], and Chihiro Kochi[1,2]

[1]Institute of Space and Astronautical Science, Japan Aerospace Exploration Agency
[2]Department of Physics, Graduate School of Science, The University of Tokyo
[3]National Astronomical Observatory of Japan
[4]Institute of Astronomy and Astrophysics, Academia Sinica

E-mail: s-baba@ir.isas.jaxa.jp

(Received February 19, 2015; Revised October 17, 2016; Accepted October 17, 2016)

ABSTRACT

The Infrared Camera onboard the *AKARI* satellite carried out spectroscopic observations with a grism mode named *NG*, whose wavelength coverage was 2.5–5.0 μm. We reinvestigate the current flux calibration for the *NG* grism mode, with which calculated flux density implausibly decreases at 4.9 μm especially for red objects due to the second-order light contamination. We perform a new spectral response calibration using blue and red standard objects simultaneously. New response curves which contain both the first- and second-order light are able to separate each contribution consistently and useful for studies of red objects such as CO ro-vibrational absorption in active galactic nuclei.

Key words: infrared: general — space vehicles: instruments — techniques: spectroscopic — methods: data analysis

1. INTRODUCTION

The Infrared Camera (IRC) is one of the focal-plane instruments onboard the *AKARI* satellite (Onaka et al., 2007). The IRC consists of three channels ranging from near- to mid-infrared, all of which have capabilities of both imaging and spectroscopy. Two dispersers are installed in the near-infrared channel (prism *NP* and grism *NG*). *NG* grism is made of germanium (Ge), covers 2.5–5.0 μm, and has higher resolution ($\lambda/\delta\lambda = 120$ at 3.6 μm) than *NP* prism. An order-sorting filter is fabricated on the surface of *NG* grism and its cut-on wavelength is 2.5 μm, (Ohyama et al., 2007).

We found that the *NG* grism mode has a problem in the flux calibration; the calculated flux density implausibly decreases at 4.9 μm especially for red objects. This anomaly is attributed to the second-order light contamination overlapping with the first-order light of longer wavelengths [See the last page of "AKARI IRC Data User Manual for Post-Helium (Phase 3) Mission" (`http://www.ir.isas.jaxa.jp/ASTRO-F/Observation/IDUM/IRC_IDUM_P3_1.1.pdf`]. The correction of this contamination is useful for studies of red objects such as active galactic nuclei (AGNs) with CO ro-vibrational absorption whose band center lies at 4.7 μm in the rest frame. In this paper, we focus on observations in Phases 1 and 2 (before the exhaustion of liquid helium).

2. METHOD

2.1. Treatment of the 2nd Order Light Contamination

Each pixel receives the first- and second-order light of certain wavelengths λ_1 and λ_2, respectively. The observed signal can be assumed as a sum of the two products of the flux density and the response of the two components as

$$N = R_1(\lambda_1)F_\nu(\lambda_1) + R_2(\lambda_2)F_\nu(\lambda_2), \quad (1)$$

where N is the signal in terms of Analog-to-Digital Unit (ADU) of each pixel, R_1 and R_2 are the responses of the

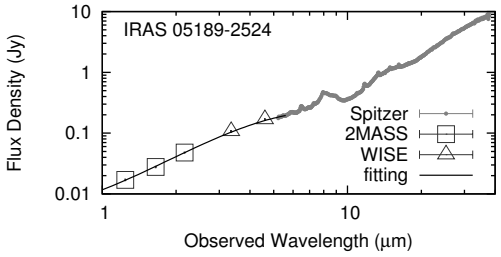

Figure 1. Flux densities of IRAS 05189-2524 from several observations. The black solid line shows a fitted cubic function, which is used as a model spectrum.

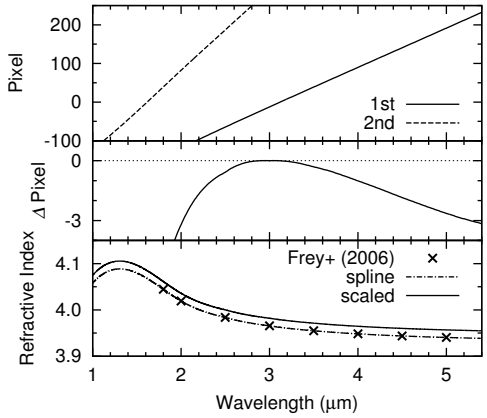

Figure 2. *Top*: Pixel-to-wavelength relation of the first- and second-order light calculated with the wavelength dependence of the refractive index of Ge. *Middle*: Difference of incident position between the linear relation used in the toolkit and this work ($\Delta\mathrm{Pixel} = \mathrm{Pixel}_{\mathrm{toolkit}} - \mathrm{Pixel}_{\mathrm{this\,work}}$). *Bottom*: Refractive index of Ge as a function of wavelength at low temperatures. The crosses represent the data in Frey et al. (2006).

first- and second-order light, and F_ν is the flux density of the object.

Since Equation (1) has two unknown responses R_1 and R_2, it cannot be solved simply by using one standard star. In order to obtain the responses of both the first- and second-order light, we apply Equation (1) to two kinds of standard objects and solve them simultaneously.

2.2. Standard Objects

As a pair of standard objects, those of blue and red spectra are preferred because they have different contribution to the amount of the contamination and the errors of the responses will become smaller.

Blue standard objects are ordinal standard stars KF09T1 and KF01T4. KF09T1 was used in the original response calibration (Ohyama et al., 2007). Model spectra of these stars are provided by Cohen (2007).

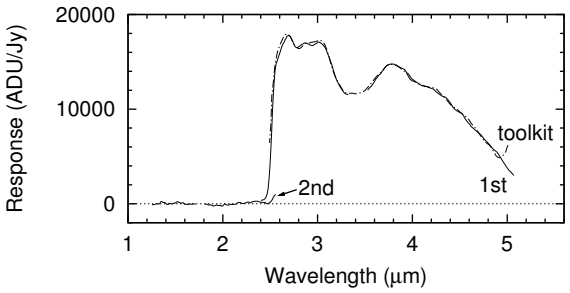

Figure 3. Response curves of *NG* grism we obtain. For comparison, the response curve of the toolkit is also shown.

We employ nearby ultra-luminous infrared galaxies (ULIRGs) IRAS 05189-2524 and Mrk 231 as the red standard objects since they have few emission and absorption features in 3–4 μm except for the 3.3 μm polycyclic aromatic hydrocarbon (PAH) emission (Imanishi & Dudley, 2000). We fit cubic functions to observational data taken with other telescopes on the $\log F_\nu$–$\log \lambda$ planes and use those curves as the model spectra of the ULIRGs assuming they have smooth spectra in the infrared except for the 3.3 μm PAH emission. An example is shown in Figure 1.

2.3. Pixel-to-Wavelength Relation

We calculate the relation between wavelength and incident position in the detector array for both the first- and second-order light considering the refractive index of Ge as a function of wavelength. Frey et al. (2006) measured the refractive index of Ge at low temperatures down to 30 K. In Phases 1 and 2, the IRC was operated at a lower temperature than 30 K (< 7 K, Nakagawa et al. (2007)). Therefore we interpolate the results tabulated in Frey et al. (2006) with a cubic spline curve and scale it so that the direct light position does not change from the current wavelength calibration of the latest IRC toolkit.

The maximum difference of the wavelength calibration between the toolkit and this work is about 0.03 μm. Figure 2 shows the refractive index of Ge and the pixel-to-wavelength relation.

3. RESULTS

We calculate the responses from two pairs of standard objects (KF09T1 and IRAS 05189-2524, KF01T4 and Mrk 231) and smooth the average of two responses. Figure 3 shows the averaged and smoothed response of *NG* grism. The response of the first-order light decreases at 4.9 μm in contrast to that of the toolkit, and that of the second-order light increase at 2.5 μm as expected.

Some points around 1.76 and 3.43 μm are the 3.3 μm PAH emission and masked in the following analysis.

4. CONCLUSIONS

We derive a new spectral response calibration for the *AKARI NG* grism mode spectroscopy to correct the second-order light contamination. The method described in this paper is promising in treating the contamination quantitatively and obtaining response curves of both the first- and second-order light simultaneously. Correct flux calibration for the wavelength of 4.9–5.0 μm is useful for studies of red objects such as AGNs with CO ro-vibrational absorption in nearby ULIRGs.

ACKNOWLEDGMENTS

We express our thanks for insightful advice and technical support to T. Shimonishi, I. Sakon, F. Usui, H. Matsuhara, T. Wada, and T. Onaka.

REFERENCES

Cohen, M. 2007, Networks of Absolute Calibration Stars for SST, AKARI, and WISE, ASP Conf. Ser., 364, 333

Frey, B. J., Leviton, D. B., & Madison, T. J., 2006, Temperature-dependent refractive index of silicon and germanium, Proc. SPIE, 6273, 62732J

Imanishi, M. & Dudley, C. C., 2000, Energy Diagnoses of Nine Infrared Luminous Galaxies Based on 3-4 Micron Spectra, ApJ, 545, 701

Nakagawa, T., Enya, K., Hirabayashi, M., et al., 2007, Flight Performance of the AKARI Cryogenic System, PASJ, 59, 377

Ohyama, Y., Onaka, T., Matsuhara, H., et al., 2007, Near-Infrared and Mid-Infrared Spectroscopy with the Infrared Camera (IRC) for AKARI, PASJ, 59, 411

Onaka, T., Matsuhara, H., Wada, T., et al., 2007, The Infrared Camera (IRC) for AKARI – Design and Imaging Performance, PASJ, 59, 401